The Plant Journal (2005) **44**, 179–194 doi: 10.1111/j.1365-313X.2005.02519.x

Cellular efflux of auxin catalyzed by the Arabidopsis MDR/PGP transporter AtPGP1

Markus Geisler[1,†], Joshua J. Blakeslee[2,†], Rodolphe Bouchard[1], Ok Ran Lee[2], Vincent Vincenzetti[1], Anindita Bandyopadhyay[2], Boosaree Titapiwatanakun[2], Wendy Ann Peer[2], Aurèlien Bailly[1], Elizabeth L. Richards[2], Karin F. K. Ejendal[3], Aaron P. Smith[2,‡], Célia Baroux[1], Ueli Grossniklaus[1], Axel Müller[4,§], Christine A. Hrycyna[3], Robert Dudler[1], Angus S. Murphy[2,*] and Enrico Martinoia[1]

[1]*Basel-Zurich Plant Science Center, University of Zurich, Institute of Plant Biology, CH-8007 Zurich, Switzerland,*
[2]*Department of Horticulture and*
[3]*Department of Chemistry, Purdue University, West Lafayette, IN 47907 USA, and*
[4]*Lehrstul für Pflanzenphysiologie, Ruhr-Universität Bochum, D-44801 Bochum, Germany*

Received 11 April 2005; revised 17 May 2005; accepted 10 June 2005.
[*]For correspondence (fax +1 765 494 0391; e-mail murphy@purdue.edu).
[†]These authors contributed equally to this work.
[‡]Present address: Department of Genetics, University of Georgia, Athens, GA, USA.
[§]Present address: Carbogen AG, C11-5001 Aarau, Switzerland.

Summary

Directional transport of the phytohormone auxin is required for the establishment and maintenance of plant polarity, but the underlying molecular mechanisms have not been fully elucidated. Plant homologs of human multiple drug resistance/P-glycoproteins (MDR/PGPs) have been implicated in auxin transport, as defects in *MDR1* (*AtPGP19*) and *AtPGP1* result in reductions of growth and auxin transport in Arabidopsis (*atpgp1*, *atpgp19*), maize (*brachytic2*) and sorghum (*dwarf3*). Here we examine the localization, activity, substrate specificity and inhibitor sensitivity of AtPGP1. AtPGP1 exhibits non-polar plasma membrane localization at the shoot and root apices, as well as polar localization above the root apex. Protoplasts from Arabidopsis *pgp1* leaf mesophyll cells exhibit reduced efflux of natural and synthetic auxins with reduced sensitivity to auxin efflux inhibitors. Expression of *AtPGP1* in yeast and in the standard mammalian expression system used to analyze human MDR-type proteins results in enhanced efflux of indole-3-acetic acid (IAA) and the synthetic auxin 1-naphthalene acetic acid (1-NAA), but not the inactive auxin 2-NAA. AtPGP1-mediated efflux is sensitive to auxin efflux and ABC transporter inhibitors. As is seen *in planta*, AtPGP1 also appears to mediate some efflux of IAA oxidative breakdown products associated with apical sites of high auxin accumulation. However, unlike what is seen *in planta*, some additional transport of the benzoic acid is observed in yeast and mammalian cells expressing *AtPGP1*, suggesting that other factors present in plant tissues confer enhanced auxin specificity to PGP-mediated transport.

Keywords: auxin, P-glycoprotein, multi-drug resistance, ABC transporter.

Introduction

Transport of the plant auxin indole-3-acetic acid (IAA) is best described by a chemiosmotic model in which plasma membrane ATPases generate an H^+ gradient between the neutral cytoplasm and the acidic extracellular space (Lomax *et al.*, 1995). Cellular IAA uptake is mediated by lipophilic diffusion of IAAH augmented by tissue-specific gradient-driven H^+ symport activity (Lomax *et al.*, 1985; Swarup *et al.*, 2004). The same gradient motivates carrier-mediated efflux of cytoplasmic anionic IAA^-. The bias of auxin transport is attributed to highly regulated, polar-localized efflux complexes characterized by the PIN-FORMED (PIN) family of facilitator proteins (Friml and Palme, 2002). PINs have been shown to align with the auxin transport vector and to be necessary for normal polarized organ development and auxin movement (Benkova *et al.*, 2003; Blilou *et al.*, 2005; Galweiler *et al.*, 1998; Palme and Galweiler, 1999). Treatment

with auxin efflux inhibitors (AEIs) phenocopies some *pin* mutant phenotypes (Friml and Palme, 2002). Additionally, some members of the PIN family exhibit vectoral relocation during tropic growth, and function in the generation and maintenance of auxin sinks (Chen *et al.*, 1998; Friml *et al.*, 2002a,b; Muller *et al.*, 1998).

Plant homologs of human multiple drug resistance/P-glycoproteins (MDR/PGPs) are numerous. The Arabidopsis PGP sub-family of ABC transporters is large, containing 21 members (five of which are highly homologous) (Jasinski *et al.*, 2003; Martinoia *et al.*, 2002). Structural characteristics of mammalian MDR/PGPs are well conserved in plant homologs, except in the predicted pore-facing helical domains thought to confer substrate specificity (Ambudkar *et al.*, 2003). Analysis of expression patterns of the 21 members of the PGP subfamily, using both the AREX and AtGENEXPRESS microarray databases, shows that members of the PGP family exhibit distinct yet overlapping expression patterns (http://www.arexdb.org/index.jsp; Schmid *et al.*, 2005).

PGPs have been implicated in auxin transport, as defects in *MDR1* (*AtPGP19*) and *AtPGP1* result in reduced growth and auxin transport of varying severity in Arabidopsis (*atpgp1*, *atpgp19*), maize (*brachytic2*/*zmpgp1*) and sorghum (*dwarf3*/*sbpgp1*) (Geisler *et al.*, 2003; Multani *et al.*, 2003; Noh *et al.*, 2001). Further, auxin transport defects and dwarf phenotypes are more exaggerated in Arabidopsis double mutants, suggesting overlapping function (Noh *et al.*, 2001). As gradient-driven anion efflux is sufficient to drive polar transport, it is not clear where plasma membrane-localized MDR/PGP ATP-binding cassette transporters fit into this scheme.

A mechanistic explanation of PGP function in auxin transport was suggested when, after fixation and detergent treatment, PIN1 was found to be mislocalized from the plasma membrane in xylem parenchyma cells of hypertropic Arabidopsis *atpgp19* hypocotyls, but not in *atpgp1* hypocotyls which do not exhibit altered tropic responses (Noh *et al.*, 2003). These results suggest that PGPs might regulate transport by stabilizing plasma membrane efflux complexes, especially as PGPs are difficult to solubilize; are localized in detergent-resistant membrane microdomains (lipid rafts); bind the non-competitive AEI 1-*N*-naphthylphthalamic acid (NPA); and are components of membrane complexes that can be dissociated by NPA treatment (Geisler *et al.*, 2003; Murphy *et al.*, 2002; Noh *et al.*, 2001). It is important to characterize the transport activity of PGPs in order to understand their functional role in these complexes.

Here we characterize the AtPGP1 protein (hereafter referred to as PGP1) by examining PGP1 localization, activity, substrate specificity and inhibition of activity. We confirm that PGP1 has an intermediate dwarf phenotype under short-day conditions, and characterize other auxin-related phenotypes. We show that PGP1 exhibits non-polar subcellular localization at the shoot and root apices that is consistent with *PGP1* expression. We show that *pgp1* mutant protoplasts exhibit reduced IAA transport, substrate specificity, and reduced sensitivity to AEIs. We show that *PGP1* expressed in yeast and the standard mammalian cell expression system used to analyze human MDR-type proteins can mediate efflux of IAA and the synthetic auxin 1-NAA, but not the weak synthetic auxin 2-NAA. Further, PGP-mediated efflux is sensitive to auxin efflux and ABC-transporter inhibitors. *PGP1* expression in yeast also results in increased resistance to toxic indolic IAA analogs. Expression of *PGP1* in mammalian cells does not enhance the efflux of other classes of compounds that are common substrates for mammalian MDR-type transporters.

Results

pgp1 *exhibits subtle auxin-related phenotypes*

While the growth phenotypes of *atpgp19* (hereafter referred to as *pgp19*) and the double mutant *pgp1 pgp19* are clearly visible in both short- and long-day conditions (Geisler *et al.*, 2003; Noh *et al.*, 2001), those of *pgp1* are not. Enhanced tropic bending observed in *pgp19* hypocotyls is not observed in *pgp1* hypocotyls (Noh *et al.*, 2003), and gravitropic defects are difficult to quantify in *pgp1* roots, largely because of greater variability in root gravitropic bending and root nutation compared with the wild type (Noh *et al.*, 2003). Reduced hypocotyl growth reported in antisense *PGP1* transformants (Sidler *et al.*, 1998) was not observed in the *pgp1* mutant (Noh *et al.*, 2001) and, in our hands and under long-day conditions, shoot and hypocotyl growth of *pgp1* mutants was difficult to distinguish from wild type (not shown). However, under shorter-day conditions, mature *pgp1* exhibited an intermediate dwarf phenotype that is not as severe as *pgp19* (Figure 1a) and is consistent with intermediate reduction in the transport of ^{3}H-IAA from the shoot apex to the root–shoot transition zone previously observed in *pgp1* (Geisler *et al.*, 2003). However, as previous assays utilizing higher concentrations of ^{14}C-IAA indicated slight increases in *pgp1* auxin transport levels (Noh *et al.*, 2001), free IAA levels in hypocotyls and whole roots of 5-day *pgp1* and *pgp19* seedlings were determined (Figure 1b) and were found to be consistent with more recently published transport data (Geisler *et al.*, 2003).

Consistent with auxin levels observed in whole-root tissues, free IAA levels in *pgp19* primary root tips were severely reduced (62 $\pm$ 18.3% of wild type). However, levels in *pgp1* root tips were lower than expected (38 $\pm$ 29.7% of wild type). A small increase in IAA leakage from *pgp1* (and not *pgp19*) root tips is also apparently a factor as, like the flavonoid-deficient mutant *tt4* (Murphy *et al.*, 2000; Peer *et al.*, 2004), *pgp1* root tips exhibited enhanced leakage of radiolabeled IAA into the support media in assays of shoot-to-root polar ^{3}H-IAA transport (124 $\pm$ 9.4% of wild-type

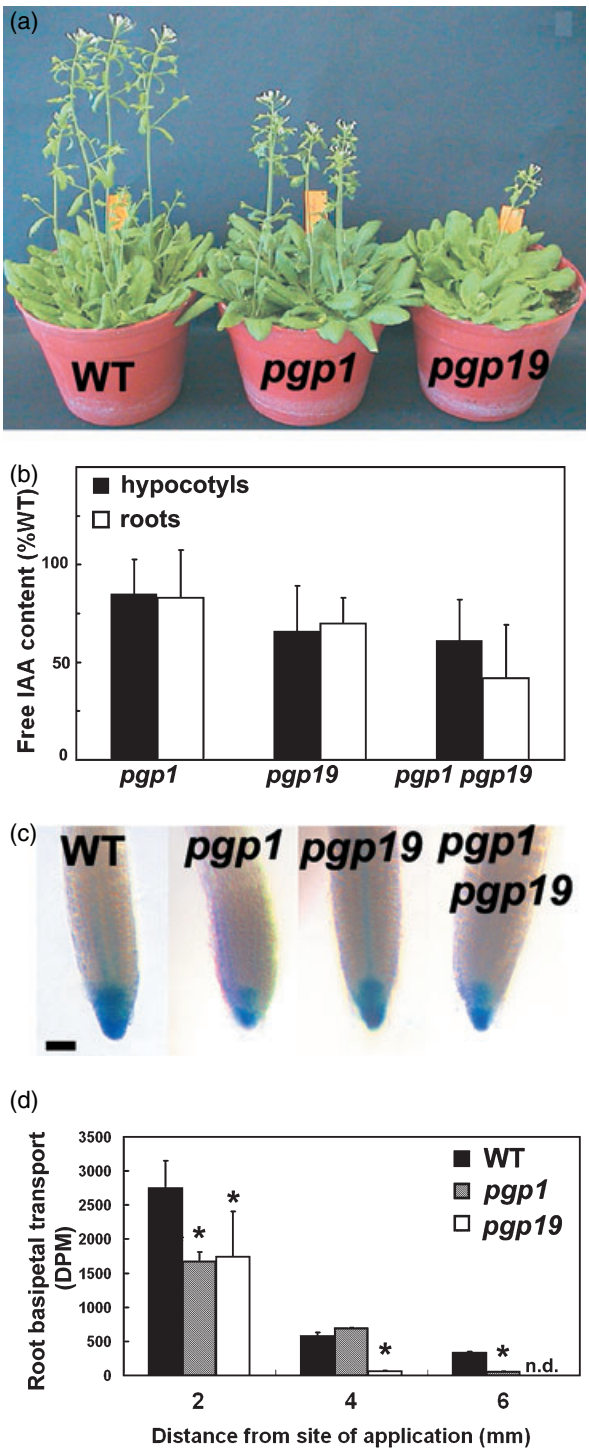

Figure 1. *pgp1* mutants have a subtle phenotype.
(a) *pgp1* and *pgp19* mutants have a dwarf phenotype under short-day conditions.
(b) Free IAA content in 5-day seedlings. Values are mean ± SD from 500 seedlings per replicate, $n = 3$. WT values = 100% ± 0.074 for hypocotyls, and 100% ± 11.114 for roots.
(c) Pro_{DR5}:GUS expression in 5-day seedling root tips. Bar, 0.1 mm.
(d) Basipetal ^{3}H-IAA transport from the root tip in 5-day seedlings. Values are mean ± SD from 10 seedlings per replicate, $n = 3$.

levels). Confirming these results, expression of the auxin reporter construct Pro_{DR5}:GUS was reduced in *pgp1*, *pgp19* and *pgp1 pgp19* compared with wild type, but was stronger in *pgp19* than in *pgp1* and *pgp1 pgp19* (Figure 1c). Additionally, a stelar Pro_{DR5}:GUS signal observed in *pgp19* was not visible in *pgp1*, consistent with a lesser accumulation of auxin in *pgp1* root tips compared with *pgp19*. The reductions of Pro_{DR5}:GUS staining observed in *pgp* mutant root tips have been further confirmed in a recently published study showing reduced Pro_{DR5}:GUS expression in the root tips of independently generated *pgp1* and *pgp19* mutants (Lin and Wang, 2005).

IAA root basipetal transport in 5-day pgp1 *seedlings*

Pro_{DR5}:GUS results suggested that basipetal transport in *pgp1* and *pgp19* might be reduced at the root tip. Consistent with these results, export of radiolabeled IAA to the 2-mm segment proximal to the root tip in *pgp1* and *pgp19* was less than in the wild type (Figure 1d). Auxin transport to the next 2-mm segment was less than wild type in *pgp19* but not *pgp1*, consistent with stronger *PGP19* expression in non-apical tissues compared with *PGP1* (Noh *et al.*, 2001; Sidler *et al.*, 1998) and greater apparent auxin retention in *pgp19*, indicated by Pro_{DR5}:GUS (Figure 1c). As PIN1 and PIN2 were not mislocalized in *pgp1* root tips (Figure 2a–d), altered PIN localization cannot account for the altered auxin transport. Application of IAA ≥2 mm above root tips of both *pgp* mutants resulted in only marginal reductions in transport compared with wild type (approximately 5% in *pgp19* and 14% in *pgp1*), suggesting limited PGP function in root basipetal transport in non-apical tissues. However, wild-type rates of basipetal auxin transport in these tissues are also much lower than apical transport rates, and decrease with distance from the root tip (data not shown). These results are similar to Pro_{DR5}:GUS activity and root basipetal transport reported in *agr1-5*/*pin2* root tips (Shin *et al.*, 2005).

PGP1 localization is non-polar at shoot and root apices

Auxin transport profiles of *pgp1* and the strong expression of *PGP1* observed in light-grown root and shoot apices (Noh *et al.*, 2001; Sidler *et al.*, 1998) focused our attention on PGP1 function in these regions. Unlike *PGP19*, which is highly expressed in upper hypocotyls and throughout the root in light-grown seedlings (Noh *et al.*, 2001), *PGP1* is expressed at lower levels in non-apical tissues in both light- and dark-grown seedlings (Geisler *et al.*, 2003; Noh *et al.*, 2001). Pro_{PGP1}:GUS enzyme and quantitative real-time PCR assays confirmed that *PGP1* expression is strongest in root and shoot apices in dark-grown wild-type seedlings (Table 1). Pro_{PGP1}:GUS visualization also confirmed previous reports of *PGP1* expression in lateral root primordia and apices (Sidler *et al.*, 1998; Figure 3c), as well as previously

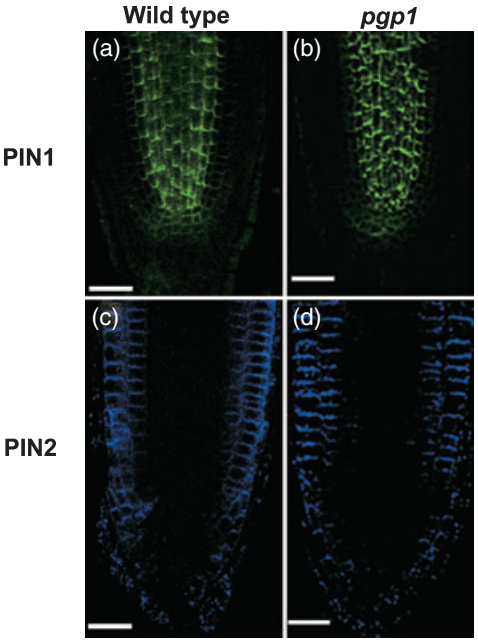

Figure 2. PIN1 and PIN2 localization is unaltered in *pgp1* root tips.
(a) PIN1 immunolocalization in 5-day wild type root tips.
(b) PIN1 immunolocalization in 5-day *pgp1* root tips.
(c) PIN2 immunolocalization in 5-day wild type root tips.
(d) PIN2 immunolocalization in 5-day *pgp1* root tips. Bar, 125 μm.

Table 1 Relative expression of *AtPGP1* in 5-day wild-type seedlings

Treatment	*AtPGP1*
Whole seedlings	
Light	1.00 ± 0.73
Light + NPA	0.60 ± 1.66
Dark	14.89 ± 0.98*
Dark + NPA	3.70 ± 1.69
Shoots	
Wild type	1.0 ± 0.8
Wild type + IAA	8.5 ± 1.4*
Roots	
Wild type	1.0 ± 0.9
Wild type + IAA	2.1 ± 0.9

NPA, 1-*N*-naphthylphthalamic acid; IAA, indole-3-acetic acid.
*Significantly different ($P < 0.05$), ANOVA followed by Tukey's *post-hoc* analysis.

unpublished weaker expression in cortical cells of the mature root and endodermal cells at the upper border of the distal elongation zone (Figure 3e). *PGP1* expression in these tissues was further confirmed by examination of original *in situ* hybridization materials from Sidler *et al.* (1998) and microarray expression data in AREX (http://www.arexdb.org/index.jsp).

PGP1 proteins were immunolocalized utilizing a functional Pro_{PGP1}:PGP1-cmyc transformant (see Experimental procedures), and the localization patterns were compared with Pro_{PGP1}:GUS expression. PGP1 exhibits a strong non-polar localization in shoot and root apical cells as well as lateral root tips (Figure 3a,b,d). This suggests a role for PGP1 in non-directional auxin export from apical cells, and suggests that PGP function may be additive to, or synergistic with, PIN protein function.

Interestingly, in root tissues above the distal elongation zone, an apparent polar PGP1 localization was observed in mature cortical and endodermal cells at the upper boundary of the distal elongation zone (Figure 3f), suggesting that PGP1 may function in polar or reflux auxin movement (Blilou *et al.*, 2005) in these tissues. In endodermal cells, the localization was always basal. In cortical cells, the localization was predominantly basal, although an apical localization without any obvious pattern was observed in some cortical cells flanking the stele. No reorientation of the basal signals was observed after microdeposition of IAA at the shoot or root tip or along the root surface (see Experimental procedures), suggesting a developmental basis for apical or basal localization. Transformation of *pgp1* with Pro_{PGP1}:PGP1-cmyc complemented the mutant phenotype and restored wild-type auxin transport profiles (Figure 4c), and PGP1 protein localization was similar to that seen in transformed wild type (Figure 3g); PIN2 localization was not altered in transformants (Figure 3h). No signal was observed in wild-type immunolocalizations utilizing only primary or secondary antibodies under any detergent-solubilization conditions; no signal was observed in transformant immunolocalizations utilizing secondary antibodies only (Figure S1).

PGP1 expression is auxin responsive

As is the case for *PGP19* (Noh *et al.*, 2001), *PGP1* expression appears to be auxin-responsive (Figure 3i,j; Table 1) and the *PGP1* promoter contains auxin response element motifs (ARFAT, ASF-1 and NtBBF1). However, *PGP1* expression in shoot tips did not expand spatially with auxin treatment (Figure 3i). *PGP1* expression was also NPA-sensitive, and NPA treatment reversed increased *PGP1* expression observed in dark-grown wild-type seedlings (Table 1).

PGP1 mediates cellular efflux in Arabidopsis protoplasts

In order to determine whether differences in auxin transport could be observed at the cellular level, efflux from protoplasts under conditions that minimize IAA catabolism was quantified. Protoplasts were isolated from leaf mesophyll cells of wild-type, *pgp1*, *pgp19* and *pgp1 pgp19* plants, but not from *pin1*, *pin2*, *pin3* or *pin4* mutants, as *PIN1*, *PIN2*, *PIN3* and *PIN4* expression is low in wild-type leaves (Figure 4a).

Wild-type protoplasts exhibited ^{3}H-IAA efflux into the media (Figure 4b), and reductions in ^{3}H-IAA efflux from *pgp*

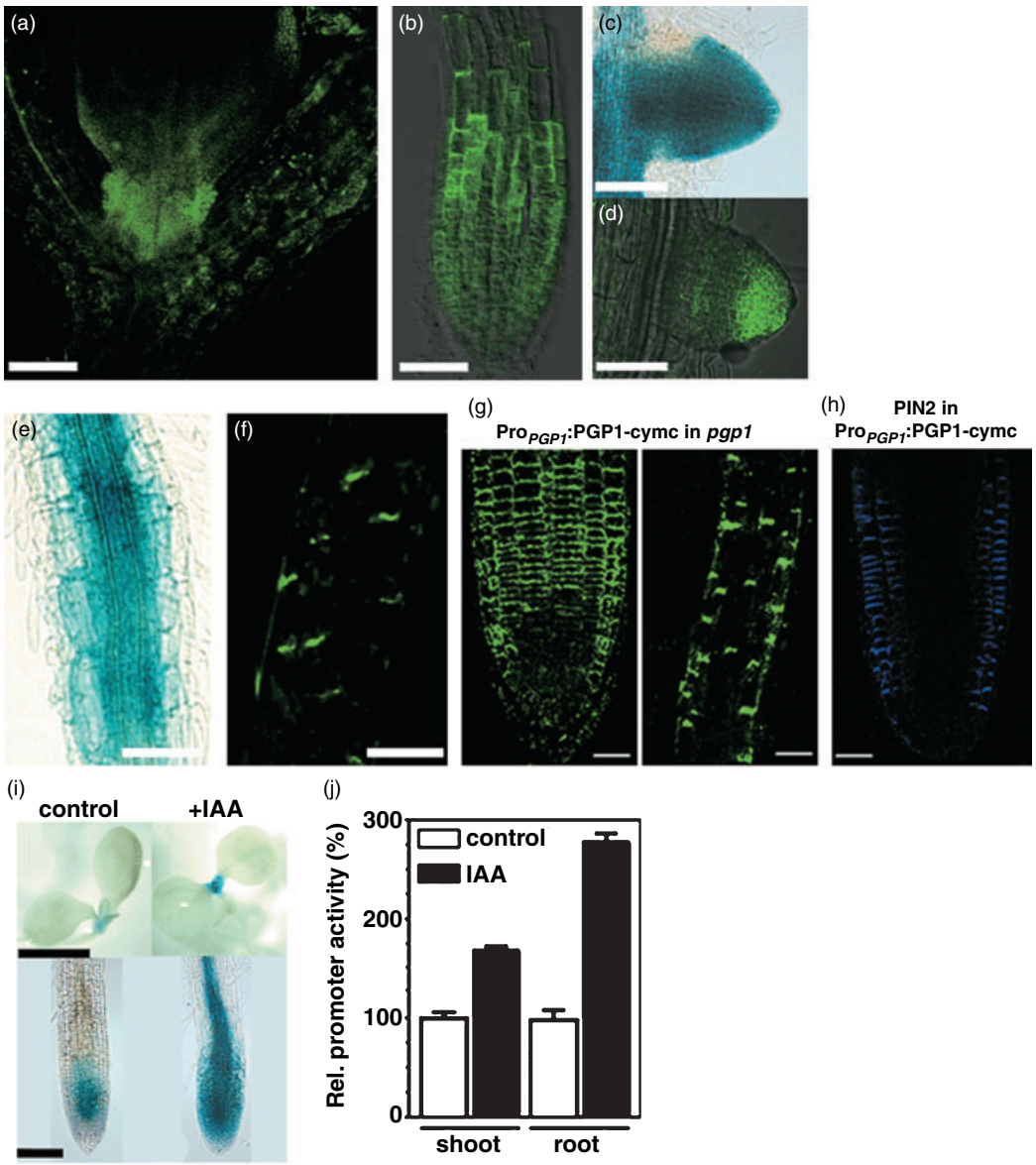

Figure 3. PGP1 localization in shoots and roots.
(a) PGP1 localization is non-polar at the shoot apex in Pro$_{PGP1}$:PGP1-cymc 5-day seedlings. Bar, 100 μm.
(b) PGP1 localization is non-polar at the root apex in Pro$_{PGP1}$:PGP1-cymc 5-day seedlings. Bar, 100 μm.
(c) Pro$_{PGP1}$:GUS is expressed in the lateral root tip in 9-day seedlings. Bar, 100 μm.
(d) PGP1 localization is restricted to the lateral root tip and a row of cells behind the lateral root tip in Pro$_{PGP1}$:PGP1-cmyc 9-day seedlings. Bar, 100 μm.
(e) Pro$_{PGP1}$:GUS is expressed in the mature root of 5-day seedlings; seedling is overstained to visualize weak cortical GUS expression. Bar, 100 μm.
(f) PGP1 localization is polar in the mature root of Pro$_{PGP1}$:PGP1-cymc 5-day seedlings. Bar, 100 μm.
(g) When *pgp1* is transformed with Pro$_{PGP1}$:PGP1-cmyc, the localization of the protein is consistent with the localization of the *in situ* hybridization and Pro$_{PGP1}$:GUS expression previously published (Sidler *et al.*, 1998) and that observed in wild type transformants. Bars, 125 and 70 μm, respectively.
(h) PIN2 localization is not different from wild type in Pro$_{PGP1}$:PGP1-cmyc transformants. Bar, 125 μm.
(i) Pro$_{PGP1}$:GUS expression increases at the shoot and root apices after 10-day seedlings are treated with 2 μM auxin (+IAA). Bar, 5 mm shoots, 0.2 mm roots. The seedlings were stained for identical amounts of time.
(j) Relative promoter activities in Pro$_{PGP1}$:GUS transformants with and without 1 μM IAA treatment.

protoplasts compared well with transport reductions seen in whole plants: 72% in *pgp1*; 57% in *pgp19*; 49% in *pgp1 pgp19* (Figure 4b). *pgp1* mutants transformed with Pro$_{PGP1}$:PGP1-cmyc had efflux levels similar to wild type (Figure 4c). Vacuolar pH, relative protoplast volume and surface area, and chloroplast number per protoplast did not differ significantly between wild-type and *pgp* protoplasts, excluding indirect effects such as vacuolar trapping (Table 2).

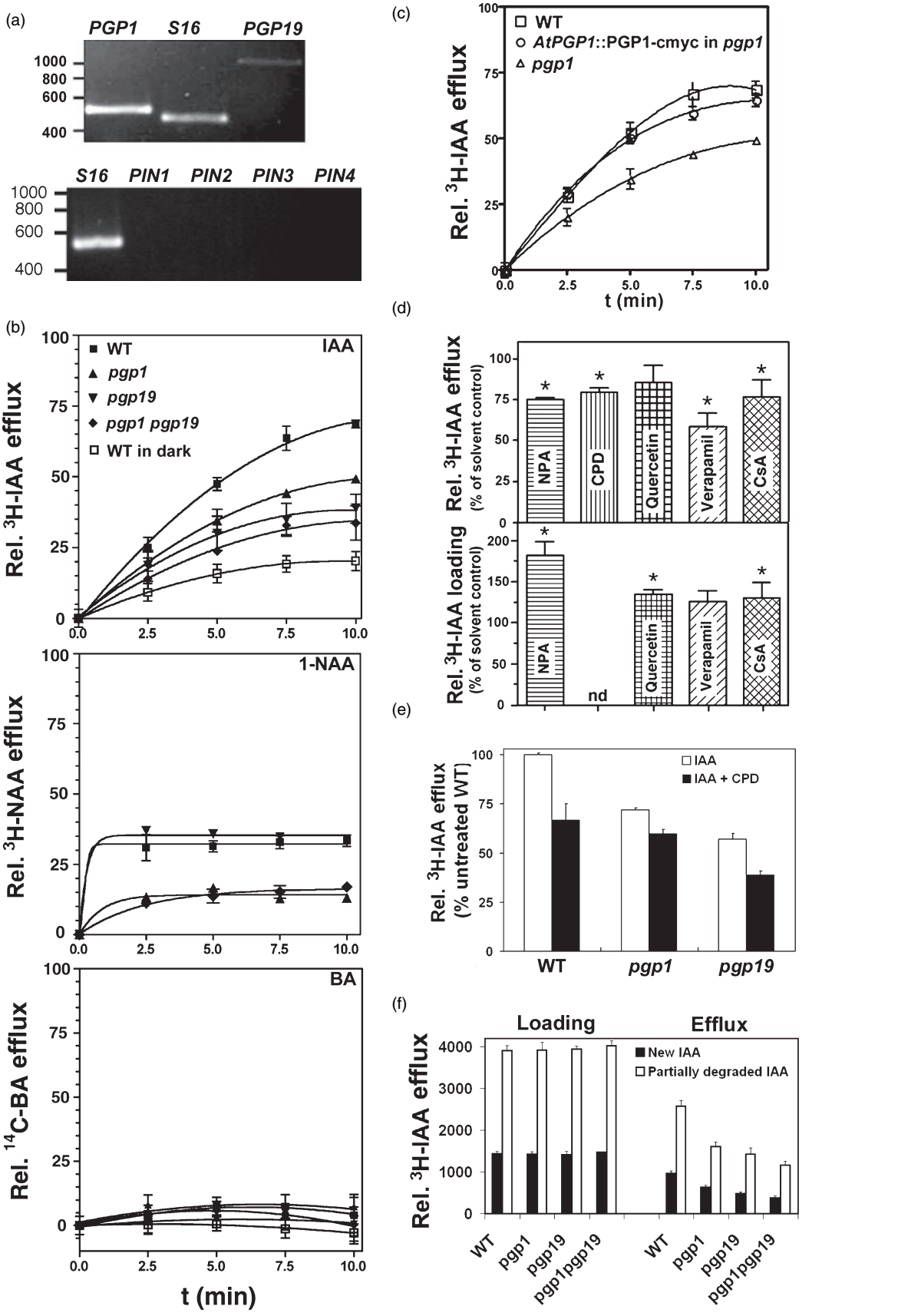
(a)
PGP1
S16
PGP19
1000
800
600
400
S16
PIN1
PIN2
PIN3
PIN4
(b)
WT
pgp1
pgp19
pgp1 pgp19
WT in dark
IAA
1-NAA
BA
Rel. 3H-IAA efflux
Rel. 3H-NAA efflux
Rel. 14C-BA efflux
t (min)
(c)
WT
AtPGP1::PGP1-cmyc in pgp1
pgp1
Rel. 3H-IAA efflux
t (min)
(d)
Rel. 3H-IAA efflux (% of solvent control)
Rel. 3H-IAA loading (% of solvent control)
NPA
CPD
Quercetin
Verapamil
CsA
nd
(e)
IAA
IAA + CPD
Rel. 3H-IAA efflux (% untreated WT)
WT
pgp1
pgp19
(f)
Loading
Efflux
New IAA
Partially degraded IAA
Rel. 3H-IAA efflux
WT
pgp1
pgp19
pgp1pgp19

Table 2 Vacuolar pH and morphological features of leaf mesophyll protoplasts

	Protoplast characteristics			
Line	Vacuolar pH	Relative volume	Relative surface area	Number of chloroplasts
Wild type	6.40	1	1	37 ± 9
pgp1	6.31	0.976 ± 0.031	0.949 ± 0.015	40 ± 9
pgp19	6.19	0.998 ± 0.028	0.919 ± 0.020	36 ± 5
pgp1 pgp19	6.04	0.724 ± 0.053*	0.514 ± 0.058*	37 ± 9

*Significantly different from wild type ($P < 0.05$), ANOVA followed by Tukey's *post-hoc* analysis.

Consistent with ATP dependence of the process, auxin efflux was diminished in protoplasts isolated from plants kept in the dark for 24 h (ATP-depleted) (30% of light-grown wild type; Figure 4b).

The synthetic auxin 1-NAA was exported by wild-type and *pgp19* protoplasts, but not *pgp1* or *pgp1 pgp19* protoplasts (Figure 4b), suggesting that PGP1 transports this synthetic auxin better than PGP19. Substrate specificity in the protoplast system was investigated further using radiolabeled benzoic acid (^{14}C-BA), a weak acid commonly used as a poorly transported control in plant assays. Negligible efflux of ^{14}C-BA out of wild type, *pgp1*, *pgp19*, *pgp1 pgp19*, and ATP-depleted wild-type protoplasts was observed (Figure 4b), demonstrating that IAA efflux from protoplasts reflects the specific auxin transport observed in whole plants.

As the AEI NPA binds MDR/PGPs (Murphy *et al.*, 2002; Noh *et al.*, 2001), and NPA treatment disrupts membrane protein complexes containing PGPs (Geisler *et al.*, 2003), IAA efflux from wild-type protoplasts would be expected to be NPA-sensitive, and *pgp* mutant protoplasts would be expected to exhibit diminished NPA sensitivity. However, an inactivating NPA amidase activity associated with the membrane aminopeptidase AtAPM1 (Katekar and Geissler, 1979, 1980; Katekar *et al.*, 1981; Murphy and Taiz, 1999a,b; Murphy *et al.*, 2002) is present in Arabidopsis leaves and is particularly active in leaf protoplasts (Murphy *et al.*, 2002; Table 3). Treatment with NPA would be expected to increase initial ^{3}H-IAA loading, but to be less effective in inhibiting ^{3}H-IAA efflux. Treatment with NPA resulted in an 82% increase in ^{3}H-IAA loading of wild-type protoplasts (Figure 4d), but only a 24% decrease in efflux. Consistent with even higher levels of NPA amidase activity in protoplasts derived from *pgp1* and *pgp19* (Table 3), measurements of NPA efflux inhibition from *pgp* protoplasts were highly variable.

Table 3 1-*N*-naphthylphthalamic acid (NPA) hydrolysis in *pgp1*/*pgp19* protoplasts: NPA hydrolysis is rapid in *pgp* mutant protoplasts compared with wild-type protoplasts

	α-Naphthylamine formation (naphthylamine equivalents)	
Time (min)	Wild type	*pgp1*/*pgp19*
0	ND	ND
5	0.4 ± 0.91	3.2 ± 0.51
10	2.6 ± 2.21	6.8 ± 1.20
15	4.7 ± 2.34	7.1 ± 2.03

Chorophyll-normalized protoplast solutions were incubated with 20 μM NPA. α-Naphthylamine was determined as described previously (Murphy and Taiz, 1999a).
ND, not determined.

However, when the non-hydrolysable NPA analog cyclopropyl propane dione (CPD) was substituted for NPA in wild-type protoplast assays, mean ^{3}H-IAA efflux was reduced approximately 30% (Figure 4e). In contrast, CPD inhibited ^{3}H-IAA transport from the tips of intact young Arabidopsis

Figure 4. Cellular auxin efflux by PGPs reflects *in planta* auxin transport.
(a) RT-PCR of 40S ribosomal protein *S16* (At2g09990), *PGP1* and *PGP19* (top) and *PIN1*, *PIN2*, *PIN3* and *PIN4* (bottom) in wild type leaf mesophyll protoplasts.
(b) ^{3}H-IAA efflux from wild type (WT) leaf mesophyll protoplasts and reduced efflux from *pgp1*, *pgp19*, *pgp1 pgp19* and dark-treated wild type leaf mesophyll protoplasts. ^{3}H-1-NAA efflux was reduced in *pgp1* and *pgp1 pgp19* compared with wild type. No efflux of ^{14}C-BA was observed. Maximum loading of the cells is set at 100%. Values are mean activities ± standard errors from three to five individual measurements, $n = 4$.
(c) Pro$_{PGP1}$:PGP1-cmyc functionally complements *pgp1*. When *pgp1* is transformed with Pro$_{PGP1}$:PGP1-cmyc, auxin efflux from in leaf mesophyll protoplasts is not different from wild type.
(d) ^{3}H-IAA efflux from Arabidopsis wild type protoplasts was significantly reduced by inhibitors of auxin efflux and mammalian MDRs. ^{3}H-IAA efflux from protoplasts (upper panel) and loading into cell suspension cultures (lower panel) in the absence (solvent control) or presence of 10 μM of indicated inhibitors was determined after 10 min. Inhibitors assayed were: 1-*N*-naphthylphthalamic acid (NPA), 1-cyclopropyl propane dione (CPD), quercetin, verapamil, and cyclosporin A (CsA). Values are mean ± standard deviations (error bars) of three individual measurements, four samples each; export statistically different (Mann–Whitney *U*-test, $P < 0.05$) compared with solvent controls is indicated by an asterisk. n.d., not determined.
(e) ^{3}H-IAA efflux from wild-type, *pgp1* and *pgp19* protoplasts is reduced by the non-hydrolyzable inhibitor cyclopropyl propane dione (CPD). ^{3}H-IAA efflux in the absence and presence of 10 μM CPD was determined after 10 min. Values are mean activities ± standard deviations (error bars) of three individual experiments, four samples each. $P > 0.05$ for *pgp1*.
(f) Inclusion of partially degraded ^{3}H-IAA resulted in increased loading of labeled IAA in wild type and *pgp* mutant protoplasts. Apparent rates of efflux appeared to increase as well. However, the relative reduction of efflux seen with fresh ^{3}H-IAA effluence observed in *pgp* mutant protoplasts remained the same.

rosette leaves approximately 40% (not shown), suggesting that structural characteristics of intact tissues not present in protoplasts contribute to NPA/CPD sensitivity. Low levels of *PIN* expression in leaf protoplasts (Figure 4a) suggest that lower abundance of PIN proteins in mesophyll tissues may be involved in this reduction of AEI sensitivity. As expected, ^{3}H-IAA efflux from CPD-treated protoplasts decreased approximately 12% in *pgp1* and approximately 20% in *pgp19* compared with the respective untreated protoplasts (Figure 4e). These results suggest that PGP19 is less sensitive than PGP1 to AEIs such as NPA and CPD, but also confirms that NPA/CPD inhibition requires factors that are altered in protoplasts.

The strong localization of PGP1 in apical tissues suggests that PGPs might also transport IAA breakdown products produced in these tissues (Kerk *et al.*, 2000). Unlabeled, presumably partially degraded IAA is often included in whole-plant radiolabeled auxin transport assays as it enhances measurable transport, possibly by enhancing uptake (Rashotte *et al.*, 2000). Protoplast assays were repeated using either >99% radiolabeled IAA or a 1:1 mixture of IAA and IAA oxidative breakdown products (primarily oxindole-acetic acid and indoleacetaldehyde, as determined by LC/MS and GC/MS). Increased loading and efflux was observed with the mixture (Figure 4f), but relative efflux from wild-type and *pgp* mutant protoplasts at 10 min was similar with both treatments. These results suggest that, in leaf cells, uptake and efflux of some IAA metabolites may be mediated by a PGP-dependent mechanism. However, it is not clear how far the specificity of IAA efflux might be enhanced in tissues where *PIN*s are strongly expressed.

Analysis of PGP1 *and auxin efflux in yeast*

Heterologous expression of *PIN2* in yeast was previously used to demonstrate a positive impact on net auxin efflux (Chen *et al.*, 1998). Although PGP19 was found to be mistargeted when expressed in a *Saccharomyces cereviseae* deletion strain (JK93da) with reduced ABC transporter activity (Noh *et al.*, 2001), immunohistochemical analyses indicated that *PGP1* expressed in JK93da strain was localized in the plasma membrane (Figure 5a). Yeast expressing *PGP1* exhibited time-dependent loading and efflux of radiolabeled IAA, 1-NAA and BA (Figure 5b). ^{3}H-IAA efflux was temperature- and glucose-dependent (Figure S2a,b); membrane permeability was unaltered (Figure S2c); and the effluent species was determined by GC-MS to be ^{3}H-IAA (Figure 5d). Efflux of ^{3}H-IAA was seven times greater in *PGP1*-transformed yeast than in vector controls, and efflux of ^{3}H-1-NAA was also slightly increased (Figure 5b). However, although no efflux of the weak synthetic auxin 2-NAA was seen (Figure 5c), a lack of specificity was indicated when efflux of ^{14}C-BA was seen to be almost equal to that of ^{3}H-IAA (Figure 5b).

Consistent with PGP1 mediation of auxin efflux, ^{3}H-IAA efflux in PGP1-transformed yeast was significantly reduced by treatment with NPA, the mammalian MDR/PGP inhibitors cyclosporin A and verapamil, and the inhibitor of both auxin transport and mammalian MDR/PGPs, quercetin (Figure 5e). Further, expression of PGP1 in the hypersensitive *gef1* yeast mutant exhibited increased resistance to the cytotoxic IAA analog 5-fluoroindole which could be reversed by both AEIs and ABC transport inhibitors (M.G., unpublished data). Additionally, yeast *yap1-1* mutants, which are hypersensitive to IAA due to increased expression of AUX1-like permeases (Prusty *et al.*, 2004), are rescued by AtPGP1 but not by mouse MDR3 (Raymond *et al.*, 1992) when grown on IAA (Figure 5f).

Analysis of PGP1*-mediated auxin efflux in mammalian cell lines*

Vaccinia virus/T7 RNA polymerase expression in human HeLa cells has become a standard system for assaying mammalian PGPs, as it provides efficient heterologous expression of functional eukaryotic plasma membrane proteins and suppression of host-protein synthesis (Elroy-Stein and Moss, 1991; Hrycyna *et al.*, 1998; Moss, 1991). Protocols to confirm protein functionality and to assay net accumulation of radiolabeled and fluorescent substrates are well established (Hrycyna *et al.*, 1998). These protocols were modified to allow loading of ^{3}H-IAA into HeLa cells while maintaining cell viability and substrate integrity.

Figure 5. Heterologous expression of *PGP1* in yeast cells results in auxin efflux.
(a) PGP1-transformed yeast express and correctly target PGP1 to the plasma membrane. Western blot of microsomes from transformed yeast: lane 1, PGP1; lane 2, vector control. Confocal analysis with anti-AtPGP1 antibody (green) and DAPI-stained nucleus (blue) (top), DIC image (bottom). Several hundred yeast cells were examined and >90% showed the pattern. Bar, 5.6 μm.
(b) Yeast cells (strain JK93da,with reduced endogenous ABC transporter activity) expressing *PGP1* effluxed ^{3}H-IAA, ^{3}H-1-NAA, and ^{14}C-BA compared with empty vector control. Mean activities ± standard errors, three to five individual measurements, $n = 4$. Values presented are relative to the total amount of radiolabeled IAA present in the media.
(c) No efflux of 2-NAA was observed in yeast cells expressing *PGP1*.
(d) MS/MS analysis of $^{13}C_6$-IAA effluent by yeast.
(e) ^{3}H-IAA efflux by yeast cells expressing *PGP1* was significantly reduced by auxin transport inhibitors and inhibitors of mammalian MDRs. Inhibitor concentrations were 10 μM. Solvent controls were set at 100%. Values presented are relative to total loading at time 0. Mean activities ± standard errors, three to five individual measurements, $n = 4$.
(f) AtPGP1, but not mouse MDR3, functionally rescued a *yap1-1* mutant strain. 10-fold dilutions of yeast cells transformed with AtPGP1 (lane 2), MmMDR3 (lane 4) or corresponding vector controls pNEV (lane 1) and pVT (lane 3) were spotted on control plates or plates supplemented by 10 μM IAA.

HeLa cells expressing *PGP1* exhibited significant ^{3}H-IAA efflux compared with empty vector controls (Figure 6a). Although loading of ^{3}H-1-NAA was less than that seen with ^{3}H-IAA, cells expressing *PGP1* exhibited a small net efflux of ^{3}H-1-NAA (Figure 6a). Cells expressing *PGP1* exhibited significant ^{3}H-IAA efflux compared with cells transformed with empty vector alone over a sixfold concentration range (Figure 6a,b). No net efflux of 2-NAA could be detected in cells expressing *PGP1* (Figure 6c). However, as seen when PGP1 was expressed in yeast, PGP1-mediated net ^{3}H-BA efflux was also observed when ^{3}H-BA was supplied at higher concentrations (Figure 6b). Background efflux of ^{3}H-BA in

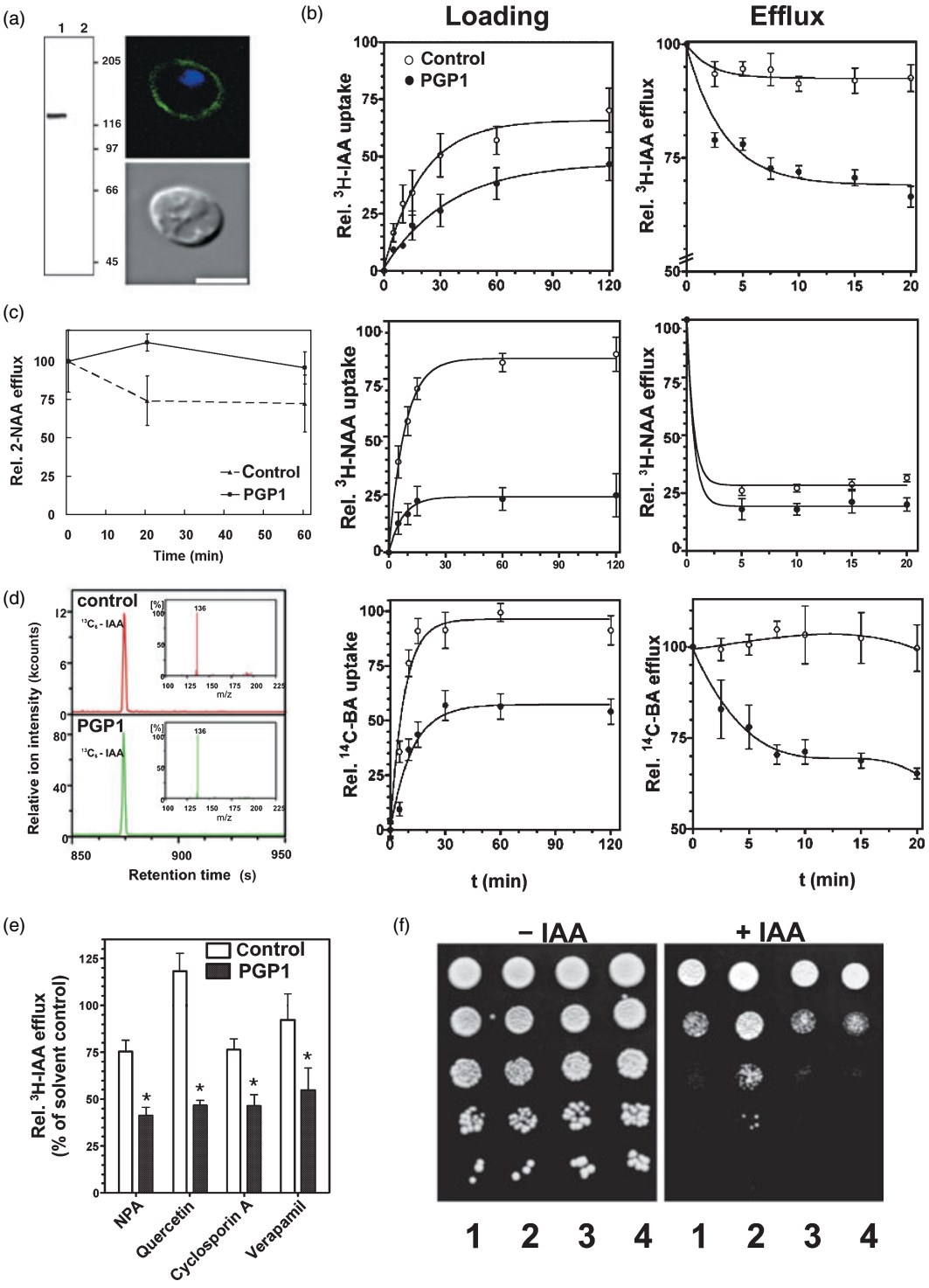

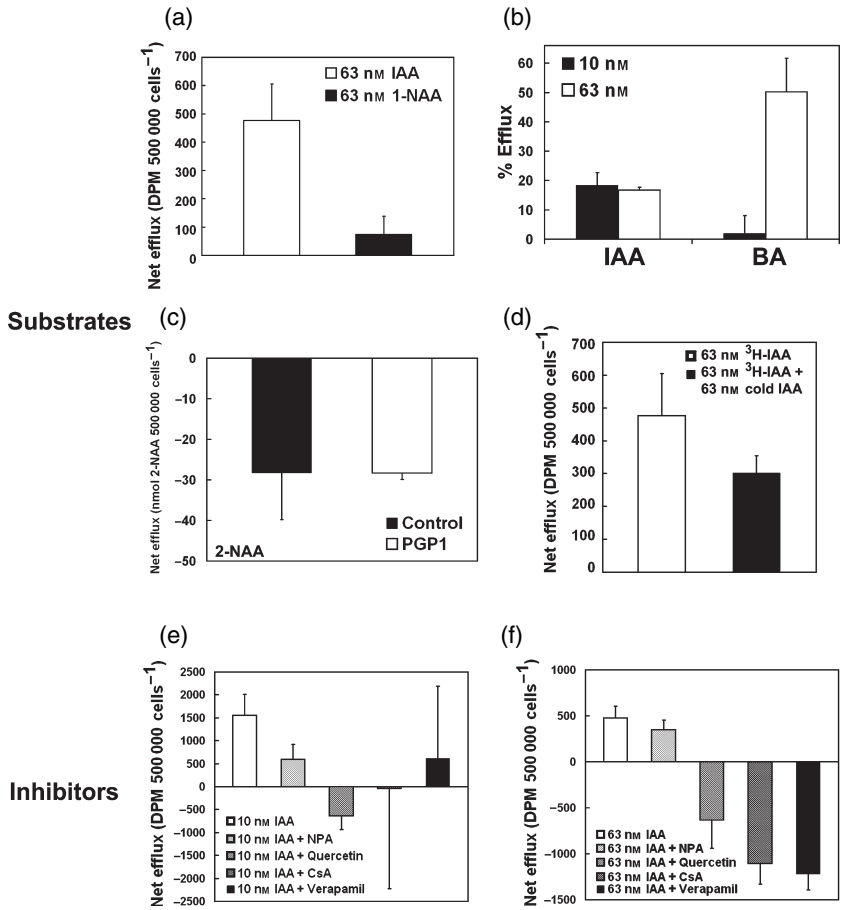

Figure 6. Efflux of radiolabeled substrates from HeLa cells expressing *PGP1*. Net efflux is expressed as DPM/500 000 cells: the amount of auxin retained by cells transformed with empty vector minus the amount of auxin retained by cells transformed with gene of interest. Reductions in auxin retention (efflux) in transformed cells are presented as positive values, while increases of auxin retention are presented as negative values. In all cases, expression and localization of expressed Arabidopsis proteins were confirmed by RT-PCR (Blakeslee *et al.*, 2004) and Western blotting (Hrycyna *et al.*, 1998) using standard protocols for the system. Cell viability after treatment was confirmed visually and via cell counting. Data points were normalized to the average empty control vector value of 2851.885 DPM/500 000 cells for auxin treatments. Means with sum standard deviations, $n = 3$.

(a) ^{3}H-IAA efflux was increased in HeLa cells expressing *PGP1*. PGP1 also modulated efflux of 1-napthalene acetic acid (^{3}H-1-NAA) and benzoic acid (^{3}H-BA).

(b) ^{3}H-IAA efflux remained constant over a sixfold concentration range in cells expressing *PGP1*. Cells expressing *PGP1* transport BA only at high concentrations. Values are presented as percent efflux of empty vector control.

(c) 2-NAA was retained in HeLa cells expressing *PGP1*. Cells were incubated with 62.59 nM cold 2-NAA. 2-NAA levels were measured via LC-MS. Data are presented in nanomoles 2-NAA/500 000 cells ± SD, and represent values obtained from two experiments, three replicates each.

(d) Unlabelled auxin degradation products competitively inhibit PGP1-modulated efflux. HeLa cells expressing *PGP1* were incubated with a 1:1 mixture of 50.3% ^{3}H-IAA and oxidative IAA breakdown products (20.4% ^{3}H-oxindole-3-acetic acid, 16.8% ^{3}H-oxindole-3-carbinol, 5.7% ^{3}H-indole-3-aldehyde, and 6.8% ^{3}H-methylene oxindole, by LC-MS/MS).

(e) ^{3}H-IAA efflux by PGP1 was inhibited by treatment with 10 μM NPA, 200 nM quercetin and by the ABC transport inhibitors cyclosporin A (CsA) and verapamil.

(f) ^{3}H-IAA efflux by PGP1 was inhibited by treatment with 10 μM NPA, 200 nM quercetin and by the ABC transport inhibitors cyclosporin A (CsA) and verapamil when cells were loaded with 10 nM radiolabeled substrate.

empty vector controls was higher than with ^{3}H-IAA, presumably due to endogenous mammalian benzoate/monocarboxylic acid transport activity (Yan and Taylor, 2002). Expression of *PGP1* in HeLa cells resulted in more auxin substrate specificity than when *PGP1* was expressed in yeast, as PGP1-mediated net efflux of ^{3}H-BA decreased to zero when ^{3}H-BA concentration was reduced to 10 nM, while ^{3}H-IAA efflux was unaffected (Figure 6b). Competition assays utilizing 10× more unlabeled BA than ^{3}H-IAA resulted in substantial inhibition of background ^{3}H-IAA efflux (data not shown), and ^{3}H-IAA efflux was reduced 22 ± 12.5% less in cells expressing *PGP1* than in empty vector controls. This suggests that background IAA efflux in HeLa cells is mediated by a monocarboxylic acid transporter, and that PGP1 is a functional IAA transporter when expressed in HeLa cells. Supporting this conclusion, the monocarboxylate transport inhibitor cardio green reduced background but not PGP1-mediated efflux (not shown).

All the assays were conducted in a buffer solution containing 1–2 mM citrate (see Experimental procedures),

indicating that organic acids such as citrate and malate are not substrates for PGP1-mediated transport. Further, no efflux of mammalian MDR/PGP hydrophobic substrates (rhodamine 123, daunomycin, BODIPY-vinblastine) was seen in cells expressing *PGP1* (Figure S3a–d). These results indicate that PGP1-mediated efflux is specific for active auxins and, to a lesser extent, a subset of aromatic carboxylic acids.

PGP1-mediated efflux of IAA oxidative degradation products in HeLa cells

As protoplast assays suggested that PGP1 may also be involved in efflux of IAA oxidative degradation products (Figure 4f), HeLa cells expressing PGP1 were incubated with a 1:1 mixture of ^{3}H-IAA and oxidative IAA breakdown products. Consistent with protoplast results, incubation of cells with 10 nM (indole equivalents) of the mixture resulted in net loading in transfected cells to levels twice those observed when cells were loaded with 63 nM fresh IAA. PGP1-mediated net ^{3}H-IAA efflux was also twice as high with this treatment (Figure 6d), but, NPA sensitivity observed at lower IAA concentrations was retained. When fresh ^{3}H-IAA was mixed with an equal amount (indole equivalents) of unlabeled oxidative breakdown products, net efflux was reduced (Figure 6d), suggesting competitive inhibition of IAA efflux. These data support a role for PGP1 in the transport of auxin breakdown products *in planta.*

Inhibitor studies of PGP1-mediated efflux in HeLA cells

The effects of inhibitor treatments on PGP1-mediated ^{3}H-IAA efflux were normalized to inhibitor-treated empty vector controls. PGP1-mediated ^{3}H-IAA net efflux was inhibited by treatment with 10 μM NPA (Figure 6e), and efflux was more NPA-sensitive at lower IAA concentrations (Figure 6e,f). Both mammalian and Arabidopsis PGPs have been shown to bind the aglycone flavonoid quercetin (Ferte *et al.*, 1999; Murphy *et al.*, 2002) which decreases mammalian PGP activity and negatively regulates auxin transport in plant tissues where PGPs are expressed (Brown *et al.*, 2001; Ferte *et al.*, 1999; Peer *et al.*, 2001, 2004). Treatment with flavonoids and mammalian MDR/PGP inhibitors has previously been shown to reverse efflux of human MDR substrates to the point of net retention in mammalian cells (Zhang and Morris, 2003). Net ^{3}H-IAA efflux by PGP1 was reversed when cells were treated with 200 nM quercetin (Figure 6e,f). Treatment with the MDR/PGP inhibitors verapamil and cyclosporin A increased net retention in cells expressing *PGP1* (Figure 6e,f), suggesting an additive cytotoxicity of these compounds in transfected cells. These data support the hypothesis that PGP1-mediated IAA transport can be regulated by endogenous flavonoids, as well as NPA. Apparently due to the background activities observed, PGP-mediated efflux exhibited reduced sensitivity to quercetin and standard MDR/PGP inhibitors at lower IAA concentrations (Figure 6e).

Discussion

Taken together, these results indicate that, in Arabidopsis, PGP1 can mediate cellular efflux of IAA and some IAA metabolites. Further, protoplast and whole-plant transport assays suggest that PGPs are capable of mediating auxin transport *in planta*, although other transport proteins may also function in auxin efflux. As PGP1-mediated auxin efflux in heterologous systems exhibits decreased specificity and AEI sensitivity, other factors present *in planta* are probably required for the high degree of specificity seen in polar auxin transport. Non-polar localization of PGP1 at root and shoot apices suggests that interactions with other proteins are also required to confer directionality to auxin transport in those tissues. In these tissues, where rediffusion of IAA exported from small cells would be expected to impair gradient-driven transport, additional energy-dependent IAA efflux might be required.

PGP1 localization and inhibition by quercetin are also consistent with its proposed interaction with endogenous flavonoids (Murphy *et al.*, 2000; Peer *et al.*, 2004). Strong expression of *PGP1* in apical tissues, localized reduction of IAA transport in the root tips of *pgp1* mutants, and PGP-mediated transport of IAA breakdown products suggest that PGP1 functions in regions exposed to high auxin concentrations. Further, the non-polar localization of PGP1 in root apices suggests that, where PIN–PGP interactions might take place, PIN proteins may confer an accelerated vectoral component to PGP-mediated transport. Specific interactions of the many PIN and PGP family members in discrete tissues would be predicted to provide tight control of transport mechanisms. To elucidate the role of PGP family members in auxin transport, further developmental and cell biological studies are required.

Experimental procedures

Plant growth conditions

Plants were grown as described previously (Geisler *et al.*, 2003). For phenotypes of adult plants, Col-0, *pgp1* (At2g36910) and *pgp19* (At3g28860) mutants were grown under short-day conditions: 8 h 100 μmol m^{-2} sec^{-1} white light, 22°C.

Expression and localization analysis

To construct the PGP1 (At2g36910) cmyc tag line (Pro$_{PGP1}$:PGP1-cmyc), a synthetic double-stranded oligonucleotide (forward primer: 5′-*ctag*agcagaagct**t**atctccgaggaggacct *ctagt*gagct; reverse primer: 5′-c*actagt*aggtcctcctcggagat**a**agcttctgct) encoding the 9E10 c-myc epitope was introduced into *Spe*I and *Sac*I sites of construct p4kbPstI (Sidler *et al.*, 1998), leading to p4kbMyc2. The cmyc

epitope is thereby inserted at amino acid residue Leu_{14}. In comparison with the original sequence, a base pair was changed (bold letter) leading to introduction of a diagnostic *Hin*dIII site (underlined) without changing the codon bias. The 5′ *Spe*I site of the oligonucleotide (italic) was designed in such a way that it was destroyed upon ligation, allowing us to use the downstream *Spe*I site (italic) for further cloning. To add the 3′-terminal part of the *PGP1* gene, a 6.7-kb *Spe*I fragment was cut out from plasmid pOE and inserted in the correct orientation into p4kbMyc2 predigested with *Spe*I, leading to pBSKMdrMyc2. From this a 9-kb *Sal*I fragment encompassing *PGP1* was subcloned into the *Sal*I site of binary plant transformation vector pBI101 (Clontech, Palo Alto, CA, USA). The final construct, PGP1cmyc2b (Pro_{PGP1}:PGP1-cmyc), containing the full-length genomic fragment of *PGP1* (including the cmyc tag at base pair 980) flanked by the *PGP1* promoter and terminator sequences, was introduced into *Arabidopsis thaliana* (ecotype Columbia) by *Agrobacteriuhm tumefaciens*-mediated vacuum infiltration. Homozygous plants were selected on 0.5× MS medium containing 50 μg ml^{-1} kanamycin, and insertion was verified by Southern analysis.

For complementation, *pgp1* mutant plants (Noh *et al.*, 2001) were transformed with the binary vector PGP1cmyc2b (Pro_{PGP1}:PGP1-cmyc) via vacuum infiltration, and homozygous lines were selected on 0.5× Murashige and Skoog (MS) medium containing kanamycin.

Arabidopsis seedlings were grown on 1% phytagar plates (0.5× MS basal salts, pH 4.85) under white light (photon flux rate 100 μmol m^{-2} sec^{-1}, 14 h light, 22°C) and 5- and 9-day seedlings were prepared for immunolocalization as described by Friml *et al.* (2003) with the following modifications: in some cases, in place of 2% driselase, 0.5 pectolyase was used for 5-day seedlings and 0.8% pectolyase for 9-day roots. Seedlings were incubated overnight (37°C) with mouse anti-cmyc antibody (Santa Cruz Biotechnology, Santa Cruz, CA, USA) at 1:250 dilution, for 3 h at 37°C with rabbit anti-mouse-FITC (whole IgG, Sigma F7506, St Louis, MO, USA) and for 3 h at 37°C with goat anti-rabbit-Alexa 488 at 1:250 in 3% BSA/MTSB, respectively. Immunofluorescence analysis was done using a confocal laser scanning microscope (Nikon, Melville, NY, USA, Eclipse 800) equipped with an argon laser (488 nm) (Bio-Rad). Images were captured with a SPOT camera and processed using Adobe PHOTOSHOP 5.0.

For histochemical GUS staining, 10-day light-grown Pro_{PGP1}:GUS transgenic seedlings were incubated in 10 mM HEPES (pH 5.2), 500 mM sorbitol containing 2 μM benzoic acid or IAA for 3 h. For all comparisons between treatments, identical staining conditions were used. For promoter gene quantification, Pro_{PGP1}:GUS transgenic seedlings were transferred for 3 h onto 0.5× MS plates supplemented with 1 μM IAA. Seedlings were washed in MS and separated manually into root and shoot, and GUS activity was assayed using 4-β-4-methylumbelliferone-glucuronide as substrate. For each sample, segments of 40 seedlings were pooled and analyzed.

Protoplast and cell culture efflux experiments

Arabidopsis mesophyll protoplasts were prepared from rosette leaves of plants grown on soil under white light (100 μmol m^{-2} sec^{-1}, 8 h light/16 h dark, 22°C). Intact protoplasts were isolated as described (Geisler *et al.*, 2003) and loaded by incubation with 1 μl ml^{-1} ^{3}H-IAA (specific activity 20 Ci $mmol^{-1}$, American Radiolabeled Chemicals, St Louis, MO, USA), 7-^{14}C-benzoic acid (53 mCi $mmol^{-1}$, Moravek Biochemicals, Brea, CA, USA) or 4-^{3}H-1-naphthalene acetic acid (25 Ci $mmol^{-1}$, American Radiolabeled Chemicals) on ice. External radioactivity was removed by separating protoplasts using a 50–30–5% percoll gradient. Samples were incubated at 25°C and efflux halted by silicon oil centrifugation. Retained and effluxed radioactivity was determined by scintillation counting of protoplast pellets and aqueous phases. For inhibitor studies, protoplasts were isolated and assayed in the presence of 10 μM of indicated inhibitors or the solvent alone.

Efflux experiments were performed with three to five independent protoplast preparations with four replicas for each time point. Protoplast volumes were determined by the addition of 0.05 μCi ^3H_2O in separate assays; protoplast surfaces were calculated by measuring protoplast diameters. Vacuolar pH was determined directly from homogenated whole leaves following centrifugation.

For inhibitor studies, 50 ml Arabidopsis cell suspension culture (May and Leaver, 1993) was grown in MS basal medium supplemented with 3% sucrose (w/v), 0.5 mg l^{-1} naphthalene acetic acid, and 0.05 mg l^{-1} kinetin in the presence of 10 μM of indicated inhibitors or the solvent alone for 12 h. Prior to measurements, the culture was centrifuged for 10 min at 115 ***g*** and 4°C, washed with sterile water and resuspended in 10 ml MCP (500 mM sorbitol, 1 mM $CaCl_2$, 10 mM MES, pH 5.6). Then 1 μl ml^{-1} ^{3}H-IAA (specific activity 20 Ci $mmol^{-1}$, American Radiolabeled Chemicals) was added, and four 500 μl aliquots were collected after 0 and 10 min incubation at 25°C and filtered on Millipore Durapore 0.22 μm GV filters. Cylcopropyl propane dione (CPD) was obtained from Caisson Labs (Rexburg, ID, USA).

Transcript detection by RT-PCR

Total RNA from Arabidopsis wild-type protoplasts was prepared, and DNaseI (Qiagen, Valencia, CA, USA) treatment was performed with column-bound RNA. Oligo dT-primed cDNA from 1 μg total RNA was synthesized using the reverse transcription system (Promega, Madison, WI, USA). Transcripts specific for *PGP1* (At2g36910), *PIN1* (At1g73590), *PIN2* (At5g57090), *PIN3* (At1g70940), *PIN4* (At2g01420) and 40S ribosomal protein *S16* (At2g09990) were detected by conventional PCR for 30 and 35 cycles at 52°C annealing temperature. Intron-spanning PCR primers were: S16-S 5′-ggcgactcaaccagctactga; S16-AS 5′-cggtaactctt tggtaacga; PGP1-S 5′-gtcccctcaagagccgtgcttg; PGP1-AS 5′-ccatcatcgatgacagcgatc, PIN1-S 5′-tggagctcaagtgcttcgccg; PIN1-AS 5′-gagaagagttatgggcaacgc; PIN2-S 5′-cacggggtcaacgagtggagc; PIN2-AS 5′-ctgagaatatcaggatggacg; PIN3-S 5′-tgatgacaaggctgatactg; PIN3-AS 5′-gtaaatcaccacgtaatccg; PIN4-S 5′-acaacgccgttaaatatgga; PIN4-AS 5′-agaccccatttttattcagcc. Equal volumes of PCR products were separated on 2.5% agarose gels. Negative controls in the absence of enzyme in the reverse transcriptase reaction yielded no products.

RNA isolation and quantitative RT–PCR analysis

RNA isolation and quantitative RT–PCR analysis were carried out as described previously, with slight modification (Blakeslee *et al.*, 2004), using the ABI Prism 7000 Sequence Detection System (Applied Biosystems, Foster City, CA, USA) in mixtures of 10 μl TaqMan Universal PCR Master Mix containing AmpliTaq Gold DNA polymerase, AmpErase uracil-*N*-glycosylase (UNG), deoxynucleoside triphosphates with dUTP, a passive reference dye, optimized buffer components (Applied Biosystems), 500 nM each primer and optimum amount of template DNA in a total volume of 20 μl. β-*tubulin* (At5g12250) forward and reverse primers were 5′-ttcccgggtcagctcaac and 5′-ggagacgagggaaaggaatga, respectively. Primers used for the *AtPGP1* transcript were 5′-tctggcgactagctaaaatgaactc and 5′-ccacaaatgacagagcctactga. The *AtPGP19* forward primer sequence was 5′-ggaagtttgaggaatctgagctattc, and the reverse primer sequence was 5′-tcggtcagtctctgcatttga.

Transcripts specific for β-*tubulin*, *AtPGP1* and *AtPGP19* were detected by PCR; activation of AmpErase UNG (2 min, 50°C) and *Taq* polymerase (10 min, 95°C), 40 cycles of denaturation (15 sec, 95°C) and elongation (1 min, 60°C).

Analysis of IAA contents and transport

pgp1 mutants expressing the maximal auxin-inducible reporter Pro_{DR5}:GUS (Ulmasov *et al.*, 1997) were generated via crossing with wild-type Pro_{DR5}:GUS plants. Seedlings were grown for 5 days as described above and stained for GUS expression (Ulmasov *et al.*, 1997).

For endogenous free auxin quantification, seedlings were grown as previously described (Geisler *et al.*, 2003). Nine days after planting seedlings were harvested, the cotyledons excised, and seedlings cut in half at the root–shoot transition zone. Roots and shoots were collected in lots of 500, and free auxin was quantified by GC-MS as described previously (Chen *et al.*, 1988). Data presented are the averages of three lots of 500 seedlings. Auxin quantifications were confirmed by GC-MS after pentafluorobenzyl derivatization (Prinsen *et al.*, 2000).

For additional free auxin quantifications, hypocotyl and root segments of 30–50 seedlings were collected and pooled. Samples were extracted and analyzed by GC-MS. Calculation of isotopic dilution factors was based on the addition of 100 pmol $^2H_2$-IAA to each sample. In some cases, roots of 40 seedlings were divided manually into 2-, 8- and 10-mm segments from the root tip, and analyzed as described above.

Auxin transport assays on intact, light-grown Arabidopsis seedlings treated with a 0.1 μl microdroplet of 1 μM auxin at the root apical meristem, using techniques described by Geisler *et al.* (2003), and root segments of 2 mm, were collected 2, 4 and 6 mm from the root tip.

2-NAA quantification

Triplicate samples were pooled and extracted in methanol/2% HCl with shaking at 4°C for 30 min. An equal volume of diethylether/hexane (1:1) was added, samples were shaken vigorously, and the upper phase was collected. This was repeated twice. Aminopropylsilyl solid phase extraction columns (Alltech, State College, PA, USA), were preconditioned with hexane before sample extracts were added. Eluate was collected from the application of three bed volumes of diethylether/2% formic acid to the column. Samples were dried prior to resuspension in methanol/1% phosphoric acid. Samples were analyzed by LC-MS using a Waters C18 MS column on a Q-TOF Micro equipped with a collision cell and phosphoric acid lock spray for internal calibration (Waters, Bedford, MA, USA), using naphthalene as an internal standard.

Auxin metabolite characterization

IAA oxidative breakdown products were determined by LC-MS and GC-MS (Ljung *et al.*, 2002, 2005).

Yeast assays

The PGP1 cDNA was cut out from plasmid pUCcMDR (Windsor *et al.*, 2003) with *Stu*I and *Hin*cII and cloned into the Klenow filled *Not*I site of yeast shuttle vector pNEV (pNEV-PGP1). pNEV and pNEV-PGP1 were introduced into *S. cerevisiae* strain JK93da or *yap1-1* (Prusty *et al.*, 2004), and single colonies were grown in synthetic minimal medium without uracil (SD-URA), supplemented with 2% glucose. For detoxification assays, transformants grown in SD-URA to an OD_{600} of approximately 0.8 were washed and diluted to $OD_{600} = 1$ in water. Cells were 10-fold diluted five times, and 5 μl of each dilution were spotted onto minimal media plates supplemented with 10 μM IAA. Growth at 30°C was assessed after 3–5 days. Assays were performed with three independent transformants.

For loading experiments, cells were grown to $OD_{600} = 1$, washed and incubated at 30°C with combinations of 1 μl ml^{-1} 5-^{3}H-IAA (specific activity 20 Ci mmol^{-1}, American Radiolabeled Chemicals), 7-^{14}C-BA (53 mCi mmol^{-1}, Moravek Biochemicals), 4-^{3}H-1-NAA (25 Ci mmol^{-1}, American Radiolabeled Chemicals) or 1 μM 2-NAA (Sigma) in SD-URA (pH 4.5). Aliquots of 0.5 ml were taken after 0, 5, 10, 30, 60 and 120 min incubation at 30°C. For efflux experiments, cells were loaded for 10 min on ice, washed twice with cold water, and resuspended in 15 ml SD (pH 4.5). Then 0.5-ml aliquots were taken after 0, 2.5, 5, 7.5 10, 15 and 20 min incubation at 30°C.

For assaying permeabilities, yeast was grown to logarithmic phase ($OD_{600} = 1.25$), washed with water followed by fluorescein diacetate (FDA) buffer, and resuspended in 5 ml FDA buffer [50 mM HEPES-NaOH (pH 7.0), 5 mM 2-deoxy-D-glucose]. Then 10 μl 5 mM FDA was added to a 990 μl cell suspension, and aliquots were measured at 485 nm excitation and 535 nm emission. To determine the temperature dependency of efflux, loaded yeast cells were washed, divided into two aliquots and incubated at 4 and 30°C, respectively. For assaying ATP dependency of transport, yeast were grown to logarithmic phase, washed with water and FDA buffer, resuspended in 50 ml FDA buffer, and incubated for 1 h at 30°C. Cells were harvested, washed and resuspended in 10.8 ml 20 mM sodium citrate (pH 4.5). After temperature equilibration at 30°C, 1 μl ml^{-1} 5-^{3}H-IAA was added, and resuspensions were divided into two aliquots followed by addition of 0.6 ml 20% glucose to one aliquot. For inhibitor studies, yeasts were grown for 12 h prior to measurement, and assayed in the presence of 10 μM of indicated inhibitors or the solvent alone.

All aliquots were filtered on Whatman GF/C filters and washed three times with cold water, and retained radioactivity was quantified by scintillation counting. All transport experiments were performed three to five times with independent transformants, with four replicas each.

To verify the identity of effluxed IAA, yeast cells transformed with pNEV and pNEV-PGP1 were loaded with 10 μM $^2H_5$-IAA and 1 μM $^{13}C_6$-IAA in 20 mM sodium citrate (pH 4.5). Effluxed IAA was extracted by ethyl acetate and analyzed by MS-MS.

Yeast PGP1 *expression and immunolocalization*

Yeast cells transformed with pNEV and pNEV-PGP1 were grown to mid-log phase and microsomes were separated via 7.5% PAGE. Western blots were immunoprobed using anti-PGP1 antibody (Sidler *et al.*, 1998). Yeast immunolocalization was performed using standard protocols. Fixed yeast cells were incubated overnight at 30°C with rabbit anti-PGP1 antibody (Sidler *et al.*, 1998) and for 3 h with goat anti-rabbit-Alexa 488 at 1:200 in 3% BSA. Stained cells were incubated in mounting media containing 4′,6-diamidino-2-phenylindole (DAPI), and immunofluorescence analysis was done using a confocal laser scanning microscope (Leica, DMIRE2) equipped with argon (488 nm) and UV laser (410 nm). Fluorescence, differential interference contrast and DAPI images were processed using Adobe PHOTOSHOP 7.0. Vector controls showed no detectable fluorescence with anti-PGP1 antibody.

HeLa cell assays

Radiolabeled substrate accumulation assay. PGP1 (At2g36910) was expressed in mammalian HeLa cells using a vaccinia virus co-transfection system providing several advantages over other heterologous expression systems, including proper glycosylation and suppression of host-protein synthesis following vaccinia infection (Elroy-Stein and Moss, 1991). The transient vaccinia expression system was used because stable cell lines develop mutations and express other endogenous drug-resistance mechanisms. Full-length, hemagglutinin (HA)-tagged PGP1 was cloned into the multiple cloning site of the pTM1 vector (Hrycyna *et al.*, 1998). For pTM1-PGP1, a *PGP1* PCR fragment containing *Xma*I/*Bam*HI restriction sites was generated using the following primers: PGP1-S 5′-tcc ccc cgg ggc atg gat aat gac ggt and PGP1-AS 5′-cgc gga tcc agc gta atc tgg tac gtc gta agc atc atc ttc ctt aac. Assays for accumulation of radiolabeled substrates were performed according to the method described by Hrycyna *et al.* (1998), with the following modifications: cells were transfected in six-well plates with 2 μg DNA (pTM1 control vector, PGP1) per well. For radiolabeled substrate accumulation assays, gradient conditions were developed wherein radiolabeled auxin was passively accumulated by empty vector control HeLa cells without induction of cellular damage. Confluent cells were transfected in six-well plates, and 16–24 h after transfection cells were washed with 3 ml pre-warmed Dulbecco's modified Eagle's medium, 5% fetal bovine serum. Each transfection utilized 600 000–1 000 000 cells, and equal loading of wells was verified by sampled cell counts. Cell counts were determined by Coulter counting and microscopic visualization (percentage confluence). Cells were then incubated with 2 ml PBS citrate buffer pH 5.5, 5% calf sera containing either 10 or 62.5 nM of the following radiolabeled substrates: ^{3}H-IAA (specific activity 26 Ci mmol^{-1}, Amersham Biosciences, Piscataway, NJ, USA); ^{3}H-benzoic acid (specific activity 20 Ci mmol^{-1}, American Radiolabeled Chemicals); or ^{3}H-1-NAA (specific activity 20 Ci mmol^{-1}, American Radiolabeled Chemicals). Possibly due to buffer compatibility issues, it was difficult to maintain solubilization of 1-NAA in loading assays. For radiolabeled auxin degradation product assays, cells were loaded with 10 nM radiolabeled IAA breakdown products (specific activity 25 Ci mmol^{-1}, American Radiolabeled Chemicals). Cells were incubated with radiolabeled substrates for 40 min at 37°C, 5% CO_2. For inhibitor studies, cells were incubated with radiolabeled IAA in the presence of 10 μM NPA, 200 nM quercetin, 1 μM cyclosporin A or 5 μM verapamil. After incubation, cells were washed three times with 3 ml ice-cold PBS, removed from the wells by trypsinization, and added to 18 ml scintillation fluid. Samples were counted in a Perkin-Elmer scintillation counter. Components of the radiolabeled auxin breakdown product mixture were determined and quantified via LC-MS. For cold 2-NAA retention studies, cells were incubated with 62.59 nM cold 2-NAA, harvested and extracted. 2-NAA was quantified using LC-MS. As with 1-NAA, it proved difficult to keep 2-NAA solubilized for cell loading in the buffer system used. Fluorescent substrate accumulation assays were performed in the HeLa cell system as previously described (Hrycyna *et al.*, 1998).

Data points were normalized to the average empty control vector value of 2851.885 DPM/500 000 cells for auxin treatments. Cell viability after treatment was confirmed visually and via cell counting.

Western blotting of HeLa cells

HeLa cells expressing PGP1 were harvested using a rubber policeman. Proteins were isolated from cells as described previously (Hrycyna *et al.*, 1998). Proteins were separated via 7% SDS-PAGE, then transferred onto nylon membrane at 10 V, in an ice bath, overnight. After blocking with 5% non-fat dried milk in 1× PBS with 0.1% Tween 20, the nylon membrane was incubated with primary antibody for 2 h at 4°C (anti-HA, Sigma). Following washing, membranes were incubated with horseradish peroxidase-conjugated secondary antibody, and developed using the ECL chemiluminescence system according to the manufacturer's protocol (Amersham Pharmacia Biotech, Piscataway, NJ, USA).

Data analysis

Data were analyzed using PRISM 4.0b (Graphpad Software, San Diego, CA, USA). Statistical analysis was performed using SPSS 11.0 (SPSS Inc., Chicago, IL, USA) and SIGMASTAT (Systat, Point Richmond, CA, USA).

Acknowledgements

We thank V. Croy, C. Gaillard, C. Ringli and A. Hopf for technical assistance, S. Plaza for help with statistical analysis, and I. Baxter for microarray data. This publication is dedicated to M.D.R. Louma (MG) and to the memory of Kenneth Thimann (ASM and WAP). This manuscript was written by ASM, MG, JJB, WAP and EM. Experiments were conceptualized by MG, JJB, WAP, ASM and EM. Auxin transport assays – whole plant: JJB; protoplast: MG, RB, VV, AB, JJB and ASM; yeast: MG, RB, JJB and ASM; HeLa cells: JJB. Implementation of HeLa cell system for auxin transport studies: JJB, ASM, ORL, KFKE and CAH. Immunolocalizations – yeast: JJB, MG and VV; Arabidopsis PIN and PGP-cmyc: AB, BT, CB and UG. Auxin determinations – ASM, AM and ELR. Cloning of PGP1 into the pTM1 expression vector by ORL. Real-time PCR analysis of PGP1 expression in HeLa cells and whole plants by ORL and WAP. DR5::GUS/PGP reporter constructs prepared by AS and ASM; DR5::GUS assays by JJB and WAP; PGP1::GUS reporter constructs created by RD; PGP1::GUS assays by MG; PGP1-cmyc transformants created by MG. Funding: National Science Foundation (US) to ASM, National Science Foundation (SWISS) to EM.

Supplementary Material

The following supplementary material is available for this article online:

Figure S1. Anti-c-myc antibody controls.

Figure S2. *PGP1* expressed in yeast cells with reduced ABC transporter activity.

Figure S3. *PGP1* expressed in HeLa cells did not transport *Homo sapiens* Multiple Drug-Resistance (HsMDR) substrates.

References

Ambudkar, S.V., Kimchi-Sarfaty, C., Sauna, Z.E. and Gottesman, M.M. (2003) P-glycoprotein: from genomics to mechanism. *Oncogene*, **20**, 7468–7485.

Benkova, E., Michniewicz, M., Sauer, M., Teichmann, T., Seifertova, D., Jurgens, G. and Friml, J. (2003) Local, efflux-dependent auxin gradients as a common module for plant organ formation. *Cell*, **115**, 591–602.

Blakeslee, J.J., Bandyopadhyay, A., Peer, W.A., Makam, S.N. and Murphy, A.S. (2004) Relocalization of the PIN1 auxin efflux facilitator plays a role in phototropic responses. *Plant Physiol.* **134**, 28–31.

Blilou, I., Xu, J., Wildwater, M., Willemsen, V., Paponov, I., Friml, J., Heidstra, R., Aida, M., Palme, K. and Scheres, B. (2005) The PIN

auxin efflux facilitator network controls growth and patterning in Arabidopsis roots. *Nature*, **433**, 39–44.

Brown, D.E., Rashotte, A.M., Murphy, A.S., Normanly, J., Tague, B.W., Peer, W.A., Taiz, L. and Muday, G.K. (2001) Flavonoids act as negative regulators of auxin transport *in vivo* in Arabidopsis. *Plant Physiol.* **126**, 524–535.

Chen, K.H., Miller, A.N., Patterson, G.W. and Cohen, J.D. (1988) A rapid and simple procedure for indole-3-acetic acid prior to GC-SIM-MS analysis. *Plant Physiol.* **86**, 822–825.

Chen, R.J., Hilson, P., Sedbrook, J., Rosen, E., Caspar, T. and Masson, P.H. (1998) The *Arabidopsis thaliana AGRAVITROPIC 1* gene encodes a component of the polar-auxin-transport efflux carrier. *Proc. Natl Acad. Sci. USA*, **95**, 15112–15117.

Elroy-Stein, O. and Moss, B. (1991) Gene expression using the vaccinia virus/t7 RNA polymerase hybrid system. In *Current Protocols in Molecular Biology* (Ausubel, F.M., Brent, R., Kinston, R.E., Moore, D.D., Smith, J.A., Seidman, J.C. and Struhl, K., eds). Hoboken, NJ, USA: John Wiley & Sons, pp. 16.19.11–16.19.19.

Ferte, J., Kuhnel, J.M., Chapuis, G., Rolland, Y., Lewin, G. and Schwaller, M.A. (1999) Flavonoid-related modulators of multidrug resistance: synthesis, pharmacological activity, and structure–activity relationships. *J. Med. Chem.* **42**, 478–489.

Friml, J. and Palme, K. (2002) Polar auxin transport – old questions and new concepts? *Plant Mol. Biol.* **49**, 273–284.

Friml, J., Wisniewska, J., Benkova, E., Mendgen, K. and Palme, K. (2002a) Lateral relocation of auxin efflux regulator PIN3 mediates tropism in Arabidopsis. *Nature*, **415**, 806–809.

Friml, J., Benkova, E., Blilou, I. *et al.* (2002b) AtPIN4 mediates sink-driven auxin gradients and root patterning in Arabidopsis. *Cell*, **108**, 661–673.

Friml, J., Benkova, E., Mayer, U., Palme, K. and Muster, G. (2003) Automated whole mount localisation techniques for plant seedlings. *Plant J.* **34**, 115–124.

Galweiler, L., Guan, C.H., Muller, A., Wisman, E., Mendgen, K., Yephremov, A. and Palme, K. (1998) Regulation of polar auxin transport by AtPIN1 in Arabidopsis vascular tissue. *Science*, **282**, 2226–2230.

Geisler, M., Kolukisaoglu, H.U., Bouchard, R. *et al.* (2003) TWISTED DWARF1, a unique plasma membrane-anchored immunophilin-like protein, interacts with Arabidopsis multidrug resistance-like transporters AtPGP1 and AtPGP19. *Mol. Biol. Cell*, **14**, 4238–4249.

Hrycyna, C.A., Ramachandra, M., Pastan, I. and Gottesman, M.M. (1998) Functional expression of human P-glycoprotein from plasmids using vaccinia virus-bacteriophage T7 RNA polymerase system. In *Methods in Enzymology: ABC Transporters: Biochemical, Cellular, and Molecular Aspects* (Ambudkar, S.V. and Gottesman, M.M., eds). San Diego, CA, USA: Academic Press, pp. 456–473.

Jasinski, M., Ducos, E., Martinoia, E. and Boutry, M. (2003) The ATP-binding cassette transporters: structure, function, and gene family comparison between rice and Arabidopsis. *Plant Physiol.* **131**, 1169–1177.

Katekar, G.F. and Geissler, A.E. (1979) Evidence of a common mode of action for auxin transport inhibitors. *Plant Physiol.* **63**, 22.

Katekar, G.F. and Geissler, A.E. (1980) Auxin transport inhibitors. 4. Evidence of a common mode of action for a proposed class of auxin transport inhibitors – the phytotropins. *Plant Physiol.* **66**, 1190–1195.

Katekar, G.F., Nave, J.F. and Geissler, A.E. (1981) Phytotropins. 3. Naphthylphthalamic acid binding-sites on maize coleptile membrane as possible receptor-sites for phytotropin action. *Plant Physiol.* **68**, 1460–1464.

Kerk, N., Jiang, K.N. and Feldmann, K.A. (2000) Auxin metabolism in the root apical meristem. *Plant Physiol.* **122**, 925–932.

Lin, R. and Wang, H. (2005) Two homologous ABC transport proteins, AtMDR1 and AtPGP1, regulate Arabidopsis photomorphogenesis and root development by mediating polar auxin transport. *Plant Physiol.* **138**, 949–964.

Ljung, K., Hull, A.K., Kowalczyk, M., Marchant, A., Celenza, J., Cohen, J.D. and Sandberg, G. (2002) Biosynthesis, conjugation, catabolism and homeostasis of indole-3-acetic acid in *Arabidopsis thaliana*. *Plant Mol. Biol.* **50**, 309–332.

Ljung, K., Hull, A.K., Celenza, J., Yamada, M., Estelle, M., Normanly, J. and Sandberg, G. (2005) Sites and regulation of auxin biosynthesis in Arabidopsis roots. *Plant Cell*, **17**, 1090–1114.

Lomax, T.L., Mehlhorn, R.J. and Briggs, W.R. (1985) Active auxin uptake by zucchini membrane-vesicles – quantitation using electron-spin-resonance volume and delta-pH determinations. *Proc. Natl Acad. Sci. USA*, **82**, 6541–6545.

Lomax, T.L., Muday, G.K. and Rubery, P.H. (1995) Auxin transport. In *Plant Hormones: Physiology, Biochemistry, and Molecular Biology* (Davies, P.J., ed.). Dordrecht, The Netherlands: Kluwer, pp. 509–530.

Martinoia, E., Klein, M., Geisler, M., Bovet, L., Forestier, C., Kolukisaoglu, U., Muller-Rober, B. and Schultz, B. (2002) Multifunctionality of plant ABC transporters – more than just detoxifiers. *Planta*, **214**, 345–355.

May, M.J. and Leaver, C.J. (1993) Stimulation of glutathione synthesis in *Arabidopsis thaliana* suspension cultures. *Plant Physiol.* **103**, 621–627.

Moss, B. (1991) Vacinia virus – a tool for research and vaccine development. *Science*, **252**, 1662–1667.

Muller, A., Guan, C.H., Galweiler, L., Tanzler, P., Huijser, P., Marchant, A., Parry, G., Bennett, M., Wisman, E. and Palme, K. (1998) AtPIN2 defines a locus of Arabidopsis for root gravitropism control. *EMBO J.* **17**, 6903–6911.

Multani, D.S., Briggs, S.P., Chamberlin, M.A., Blakeslee, J.J., Murphy, A.S. and Johal, G.S. (2003) Loss of an MDR transporter in compact stalks of maize *br2* and sorghum *dw3* mutants. *Science*, **302**, 81–84.

Murphy, A.S. and Taiz, L. (1999a) Naphthylphthalamic acid is enzymatically hydrolyzed at the hypocotyl-root transition zone and other tissues of Arabidopsis seedlings. *Plant Physiol. Biochem.* **37**, 413–430.

Murphy, A.S. and Taiz, L. (1999b) Localization and characterization of soluble and plasma membrane aminopeptidase activities in Arabidopsis seedlings. *Plant Physiol. Biochem.* **37**, 431–443.

Murphy, A., Peer, W.A. and Taiz, L. (2000) Regulation of auxin transport by aminopeptidases and endogenous flavonoids. *Planta*, **211**, 315–324.

Murphy, A.S., Hoogner, K.R., Peer, W.A. and Taiz, L. (2002) Identification, purification, and molecular cloning of *N*-1-naphthylphthalmic acid-binding plasma membrane-associated aminopeptidases from Arabidopsis. *Plant Physiol.* **128**, 935–950.

Noh, B., Murphy, A.S. and Spalding, E.P. (2001) Multidrug resistance-like genes of Arabidopsis required for auxin transport and auxin-mediated development. *Plant Cell*, **13**, 2441–2454.

Noh, B., Bandyopadhyay, A., Peer, W.A., Spalding, E.P. and Murphy, A.S. (2003) Enhanced gravi- and phototropism in plant *mdr* mutants mislocalizing the auxin efflux protein PIN1. *Nature*, **423**, 999–1002.

Palme, K. and Galweiler, L. (1999) PIN-pointing the molecular basis of auxin transport. *Curr. Opin. Plant Biol.* **2**, 375–381.

Peer, W.A., Brown, D.E., Tague, B.W., Muday, G.K., Taiz, L. and Murphy, A.S. (2001) Flavonoid accumulation patterns of transparent testa mutants of Arabidopsis. *Plant Physiol.* **126**, 536–548.

Peer, W.A., Bandyopadhyay, A., Blakeslee, J.J., Makam, S.N., Chen, R., Mason, P. and Murphy, A. (2004) Variation in expression and protein localization of the PIN family of auxin efflux facilitator proteins in flavonoid mutants with altered auxin transport in *Arabidopsis thaliana*. *Plant Cell*, **16**, 1898–1911.

Prinsen, E., Van Laer, S., Öden, S. and Van Onckelen, H. (2000) Auxin analysis. In *Methods in Molecular Biology, Vol. 141: Plant Hormone Protocols* (Tucker, G.A. and Roberts, A., eds). Totowa, NJ, USA: Humana Press, pp. 49–65.

Prusty, R., Grisafi, P. and Fink, G.R. (2004) The plant hormone indoleacetic acid induces invasive growth in *Saccharomyces cerevisiae*. *Proc. Natl Acad. Sci. USA*, **101**, 4153–4157.

Rashotte, A.M., Brady, S.R., Reed, R.C., Ante, S.J. and Muday, G.K. (2000) Baspipetal auxin transport is required for gravitropism in roots of Arabidopsis. *Plant Physiol.* **122**, 481–490.

Raymond, M., Gros, P., Whiteway, M. and Thomas, D.Y. (1992) Functional complementation of yeast ste6 by a mammalian multidrug resistance *mdr* gene. *Science*, **256**, 232–234.

Schmid, M., Davison, T.S., Henz, S.R., Pape, U.J., Demar, M., Vingron, M., Schölkopf, B., Weigel, D. and Lohmann, J. (2005) A gene expression map of Arabidopsis development. *Nat. Genet.* **37**, 501–506.

Shin, H., Shin, H.-S., Guo, Z., Blancaflor, E.B., Masson, P.H. and Chen, R. (2005) Complex regulation of Arabidopsis AGR1/PIN2-mediated root gravitropic response and basipetal auxin transport by cantharidin-sensitive protein phosphatases. *Plant J.* **42**, 188–200.

Sidler, M., Hassa, P., Hasan, S., Ringli, C. and Dudler, R. (1998) Involvement of an ABC transporter in a developmental pathway regulating hypocotyl cell elongation in the light. *Plant Cell*, **10**, 1623–1636.

Swarup, R., Kargul, J., Marchant, A. *et al.* (2004) Structure–function analysis of the presumptive Arabidopsis auxin permease AUX1. *Plant Cell*, **16**, 3069–3083.

Ulmasov, T., Mufett, J., Hagen, G. and Guilfoyle, T.J. (1997) Aux/IAA repress expression of reporter gene containing natural and highly active synthetic auxin response elements. *Plant Cell*, **9**, 1963–1971.

Windsor, B., Roux, S. and Lloyd, A. (2003) Multiherbicide tolerance conferred by AtPgp1 and apyrase overexpression in *Arabidopsis thaliana*. *Nat. Biotechnol.* **21**, 428–433.

Yan, R. and Taylor, E.M. (2002) Neotrofin is transported out of brain by a saturable mechanism: possible involvement of multidrug resistance and monocarboxylic acid transporters. *Drug Metabol. Dispos.* **30**, 513–518.

Zhang, S.Z. and Morris, M.E. (2003) Effects of the flavonoids biochanin A, morin, phloretin, and silymarin on P-glycoprotein-mediated transport. *J. Pharmacol. Exp. Ther.* **304**, 1258–1267.